

The influence of Te-precursor in Mo-V-Te-O and Mo-V-Te-Nb-O catalysts on their catalytic behaviour in the selective propane oxidation

P. Botella, P. Concepción, J.M. López Nieto*, Y. Moreno

Instituto Tecnología Química, UPV-CSIC, Avda Los Naranjos s/n, 46022 Valencia, Spain

Available online 28 December 2004

Dedicated to Professor Ferruccio Trifirò on the occasion of his 65th birthday.

Abstract

A comparative study on the catalytic behaviour of Mo-V-Te-Nb-O and Mo-V-Te-O catalysts prepared from Te^{6+} - or Te^{4+} -containing precursors, i.e. H_6TeO_6 and TeO_2 , respectively, in the absence or in the presence of Nb oxalate and/or oxalic acid is presented. The characterization of catalysts by X-ray diffraction (XRD), diffuse reflectance and photoelectron spectra (XPS) before and after the calcination step suggests that the nature of metal precursors in the synthesis gel strongly modifies both the nature of crystalline phases and the oxidation state of reducible metals. The catalytic activity (and probably the incorporation of vanadium in the crystalline structures) is favoured by using a Te^{6+} -containing precursor and Nb oxalate or a Te^{4+} -containing precursor. However, Nb-containing catalysts present the better catalytic performance in the selective oxidation of propane to acrylic acid suggesting an important influence of the presence of Nb^{5+} cations in the catalysts on the formation and/or stability of acrylic acid.

© 2004 Published by Elsevier B.V.

Keywords: Selective oxidation of propane to acrylic acid; Mo-V-Te-Nb mixed metal oxide catalyst; Hydrothermal synthesis

1. Introduction

Mo-V-Nb-Te-O catalysts have been proposed as active and selective in the ammoxidation of propane to acrylonitrile [1–5], the selective oxidation of propane to acrylic acid [6–11], and in the oxidative dehydrogenation of ethane to ethene [12,13]. Although the catalysts are generally obtained by heat-treatment at about 600 °C in N_2 from catalyst precursors prepared by evaporation of aqueous slurries of the corresponding metal salts [1–9], hydrothermal synthesis seems to be an alternative route to achieve these catalyst precursors [10–18].

Ueda and coworkers [14,15] proposed the hydrothermal synthesis of Mo-V-Me (Me = Te, Sb) catalysts for selective oxidation of short chain alkanes. However, yields of acrylic acid of 12.4% were reported on Mo-V-Te-O catalysts prepared with TeO_2 .

Botella and coworkers [10,11,16] proposed the hydrothermal synthesis of Nb-containing Mo-V-Te-O catalysts, from gels containing vanadyl sulfate, niobium oxalate and an Anderson-type telluromolybdate [10,11] or ammonium heptamolybdate/telluric acid [16], as an alternative route to achieve active and selective catalysts for the selective oxidation of propane to acrylic acid. In this way, they reported yields to acrylic acid of 36–38% [11,16]. More recently, Grasselli et al. [5] have confirmed the high performance of catalysts prepared hydrothermally, introducing interesting topics on the functionalization of the different crystalline phases present in these catalysts.

The catalytic performance of MoVTe-based catalysts seems to be strongly influenced by the nature of Te-starting compounds and/or the presence of Nb. Thus, Mo-V-Te-Nb-O catalysts prepared hydrothermally by using Te(VI) -polyoxocompounds, i.e. Anderson-type telluromolybdate, are more active and selective to those prepared by using Te(IV) -polyoxocompounds, i.e. $(\text{NH}_4)_4\text{TeMo}_6\text{O}_{22}\cdot 2\text{H}_2\text{O}$

* Corresponding author. Fax: +34 96 3877809.

E-mail address: jmlopez@itq.upv.es (J.M. López Nieto).

[16]. So, the nature of Te-precursor seems to be an important factor in the preparation of these catalysts.

Moreover, it has been observed that Nb-containing catalysts present better yields of acrylic acid than the corresponding Nb-free catalysts [11,12,16,17], probably as a consequence of the different reaction products stabilities in the presence or in the absence of Nb in the catalyst [17].

In this paper, we present a comparative study on the catalytic behaviour of Mo-V-Te-Nb-O and Mo-V-Te-O catalysts prepared from Te^{6+} - or Te^{4+} -containing precursors, i.e. H_6TeO_6 and TeO_2 , respectively, in the absence and the presence of Nb oxalate and/or oxalic acid. The characterization of solid materials has also permitted to evaluate the changes observed in both the catalyst and the catalyst precursors depending on the Te-starting compound. The importance of the oxidation state of Te and the role of oxalic acid in the catalyst preparation are also discussed.

2. Experimental

2.1. Catalyst preparation

Mo-V-Te-O and Mo-V-Te-Nb-O catalysts have been prepared hydrothermally according to a procedure previously reported [11]. The gels, aqueous solutions of the corresponding salts, presented Mo/V/Te/Nb atomic ratios of 1/0.20–40/0.17/0–0.17. Vanadyl sulphate, ammonium heptamolybdate and niobium oxalate were used as V-, Mo- and Nb-precursors, whereas TeO_2 or H_6TeO_6 were used as Te compounds. The gels were autoclaved in teflon-lined stainless-steel autoclaves at 175 °C for 48 h. The resulting precursors were filtered, washed, dried at 80 °C for 16 h and heat-treated at 600 °C during 2 h in N_2 -stream. The characteristics of catalysts are shown in Table 1.

2.2. Catalyst characterization

BET specific surface areas were measured on a Micromeritics ASAP 2000 instrument (adsorption of krypton) and on a Micromeritics Flowsorb (adsorption of N_2).

X-ray diffraction patterns (XRD) were collected using a Philips X'Pert diffractometer equipped with a graphite monochromator, operating at 40 kV and 45 mA and employing nickel-filtered Cu $\text{K}\alpha$ radiation ($\lambda = 0.1542$ nm).

Diffuse reflectance UV–vis spectra (DRS) were collected on a Cary 5 apparatus equipped with a ‘Praying Mantis’ attachment (from Harric) under ambient conditions. $\text{TeMo}_5\text{O}_{16}$, MoO_3 , Nb_2O_5 , MgV_2O_6 , H_6TeO_6 and TeO_2 have been used as standard compounds [18].

Photoelectron spectra (XPS) were recorded on a VG-Escalab-210 Spectrometer using Al $\text{K}\alpha$ radiation (Al $\text{K}\alpha = 1486$ eV) operated at 12 kV and 20 mA. The spectrometer's hemispherical analyser was set to 50 eV constant pass energy. The samples were previously outgassed at 100 °C for 2 h in the preparation chamber of the spectrometer and subsequently transferred to the analysis chamber where the pressure during spectra acquisition was 5×10^{-10} Torr. The binding energy (BE) data were referenced to C 1s (BE = 284.5 eV). Atomic ratios of the elements were calculated from the relative peak areas of the respective core level lines using the Wagner sensitivity factors [19]. The integration of the V $2p_{3/2}$ core level line is influenced by the $\text{K}\alpha_{3,4}$ satellite of the O 1s line. Therefore, the satellite subtraction (intensity ratios III_0 and energies distances ΔE , between main line and satellite) have been adjusted by using a reference material without vanadium in order to obtain a smooth background baseline, as indicated previously [20]. By optimising the above mentioned parameters, the values obtained for the satellite subtraction are $\text{K}\alpha_3$: $III_0 = 0.06225$, $\Delta E = 9.8$ eV; and $\text{K}\alpha_4$: $III_0 = 0.030$, $\Delta E = 11.8$ eV. Data analysis procedure involve smoothing, a Shirley background subtraction and curve fitting using mixed Gaussian–Lorentzian functions by a least-squares method.

2.3. Catalytic tests

The catalytic experiments were carried out in a fixed bed quartz tubular reactor working at atmospheric pressure in the 320–420 °C temperature interval [11]. A 0.5–2.5 g of catalyst samples (0.3–0.5 mm particle size) were used in order to achieve different contact times. The samples were diluted with 2.0–4.0 g of silicon carbide (0.5–0.75 mm

Table 1
Textural and bulk characteristics of Nb-free and Nb-containing MoVTe-oxide catalysts

Sample	Te-precursor	Mo/oxalate molar ratio	S_{BET} ($\text{m}^2 \text{g}^{-1}$)	Chemical analysis ^a		Crystalline phases ^b
				As-synthesized	Heat-treated	
T4-1	TeO_2	0	7.0	$\text{Mo}_1\text{V}_{0.45}\text{Te}_{0.15}$	$\text{Mo}_1\text{V}_{0.47}\text{Te}_{0.14}$	$\text{Te}_2\text{M}_{20}\text{O}_{57}^c > \text{Te}_{0.33}\text{MO}_{3.33}^c$
T6-1	H_6TeO_6	0	6.4	$\text{Mo}_1\text{V}_{0.15}\text{Te}_{0.19}$	$\text{Mo}_1\text{V}_{0.11}\text{Te}_{0.16}$	$\text{TeMo}_5\text{O}_{16} \gg \text{Mo}_{5-x}(\text{V/Nb})_x\text{O}_{14}$
T6-1-O^d	H_6TeO_6	1.7	25.1	$\text{Mo}_1\text{V}_{0.15}\text{Te}_{0.19}$	$\text{Mo}_1\text{V}_{0.14}\text{Te}_{0.14}$	$\text{Te}_2\text{M}_{20}\text{O}_{57}^c > \text{TeMo}_5\text{O}_{16} \gg \text{Te}_{0.33}\text{MO}_{3.33}^c$
T4-2	TeO_2	1.7	10.2	$\text{Mo}_1\text{V}_{0.17}\text{Te}_{0.22}\text{Nb}_{0.15}$	$\text{Mo}_1\text{V}_{0.19}\text{Te}_{0.13}\text{Nb}_{0.19}$	$\text{Te}_2\text{M}_{20}\text{O}_{57}^c \gg \text{Te}_{0.33}\text{MO}_{3.33}^c \text{ Mo}_{5-x}(\text{V/Nb})_x\text{O}_{14}$
T6-2	H_6TeO_6	1.7	15.5	$\text{Mo}_1\text{V}_{0.25}\text{Te}_{0.23}\text{Nb}_{0.1}$	$\text{Mo}_1\text{V}_{0.18}\text{Te}_{0.13}\text{Nb}_{0.12}$	$\text{Te}_2\text{M}_{20}\text{O}_{57}^c \gg \text{Te}_{0.33}\text{MO}_{3.33}^c \text{ Mo}_{5-x}(\text{V/Nb})_x\text{O}_{14}$

^a Atomic composition was done by atomic absorption spectroscopy.

^b As determined by XRD of the heat-treated samples.

^c M = Mo and V.

^d Oxalic acid instead of Nb oxalate has been incorporated in the synthesis gel.

^e M = Mo, V and Nb.

particle size) in order to keep a constant volume in the catalyst bed. The feed consisted of a mixture of propane/oxygen/water/helium with a molar ratio of 4/8/30/58 and a total flow of $50 \text{ cm}^3 \text{ min}^{-1}$. Reactants and reaction products were analysed by on-line gas chromatography, using two Hewlett-Packard apparatus equipped with three columns: (i) 23% SP-1700 chromosorb PAW ($3.0 \text{ m} \times 1/8 \text{ in.}$) to separate hydrocarbons and CO_2 ; (ii) Carbosieve-S ($8 \text{ m} \times 1/8 \text{ in.}$) to separate O_2 and CO ; (iii) Porapak Q ($3.0 \text{ m} \times 1/8 \text{ in.}$) to separate oxygenated products. Blank runs showed that under the experimental conditions used in this work the homogeneous reaction could be neglected.

3. Results

3.1. Catalyst characterization

Table 1 presents the characteristics of catalysts. In general, the catalysts prepared in the presence of oxalate anions present a surface area higher than those prepared without them. So, oxalate anions could have an important role in the crystallinity of these catalysts [4,5,11].

Fig. 1 presents the XRD patterns of samples prepared hydrothermally, before (Fig. 1A) and after (Fig. 1B) the calcination step. Two intense peaks at $2\theta = 8.16$ and 28.56 in addition to more than 25 peaks (the most intense peaks appear at $2\theta = 16.40, 21.75, 22.63, 28.03, 28.56, 29.8$ and 31.5) are observed in the as-synthesised **T6-1** sample (Fig. 1A, pattern a). This XRD pattern is quite different to those observed in previously reported telluromolibdates (with and without V ions) [21,22]. However, the structure is still unknown.

Different XRD patterns are observed in the rest of as-synthesised samples, which present pseudoamorphous or low crystalline phase (Fig. 1A, patterns b–e). Thus, broad peaks at $2\theta = 9.0, 22.2, 27.4$ and 45.4 are mainly observed.

This could correspond to the incipient formation of an orthorhombic phase, previously described for Mo-V-Te-O [11,14] and Mo-V-Te-Nb-O [11,14,16] catalysts. Note that the XRD pattern of as-synthesised **T6-1-O** sample (Fig. 1A, pattern b), shows a crystallinity intermediate between Nb-free and Nb-containing sample (Fig. 1A, patterns a and c, respectively), suggesting that the presence of oxalic acid during the catalyst preparation plays an important role in the formation of crystalline phases, specially when using telluric acid as Te-precursor.

In the case of calcined materials, the XRD pattern of **T6-1** sample suggests the presence of $\text{TeMo}_5\text{O}_{16}$ (peaks at $2\theta = 21.7, 24.6, 26.2, 26.67, 30.5$) (JCPDS: 31-874) and a V-containing $\text{Mo}_{5-x}\text{V}_x\text{O}_{14}$ phase (peaks at $2\theta = 7.75, 8.86, 12.3, 16.46, 22.25, 23.4, 24.9, 28.1$ and 31.5) (JCPDS: 31-1437 and 12-5179) (Fig. 1B, pattern a), while the XRD pattern of the heat-treated **T6-1-O** sample (Fig. 1B, pattern b) suggests the presence of both $\text{TeMo}_5\text{O}_{16}$ and $\text{Te}_2\text{M}_{20}\text{O}_{57}$. The rest of the catalysts present XRD pattern similar to those proposed in the orthorhombic $\text{Te}_2\text{M}_{20}\text{O}_{57}$ phase [5,13,14,16,24,25], with the presence of $\text{Te}_{0.33}\text{MO}_{3.33}$ ($\text{M} = \text{Mo, V, Te}$) and V- and/or Nb-containing Mo_5O_{14} phases. These results suggest that $\text{Te}_2\text{M}_{20}\text{O}_{57}$ could be formed when using a Te^{4+} -precursor in agreement to previous results [23]. However, the formation of $\text{Te}_2\text{M}_{20}\text{O}_{57}$ is quite favoured by adding Nb-oxalate or oxalic acid when using a Te^{6+} -precursor.

Fig. 2 shows the DRS spectra of Nb-free and Nb-containing MoVTe-oxide catalysts before (Fig. 2A) and after (Fig. 2B) the calcination step. The DRS spectra of as-synthesised samples are characterized by the presence of one or two broad bands in the 200–400 nm region. The broad band in the 250–400 nm region is related to the presence of Mo^{6+} [26–28] and V^{5+} [26,27,29], although their positions depend on the Me-environment. In our case, the absorption bands in the range 290–350 and 350–450 nm can be related to the presence of Mo^{6+} and V^{5+} cations, respectively, in octahedral environment. Since molybdenum atoms in Mo-V-Te-Nb-O catalysts keep a distorted six-coordinated environment with $\text{Mo}^{6+}\text{--O--Me}$ bridges bonds ($\text{Me} = \text{Mo}^{5+}$ and/or Mo^{6+} in addition to $\text{V}^{5+}/\text{V}^{4+}$ and/or Nb^{5+}), the differences observed in the 200–400 nm region should be related to different oxidation states presented in the crystalline phases.

In addition to these, two bands centred at 560 and 650 nm with medium and low intensity, respectively, are also observed in all uncalcined samples except in **T6-1**. These results suggest the presence of Mo and V species with oxidation states lower than 6+ and 5+, respectively, in most of the uncalcined samples.

Similar spectra are observed in heat-treated samples although the intensities of the bands in the 200–400 nm region decrease and those in the 500–700 nm region increase (Fig. 2B). It has been reported that the band in the 500–600 nm region may be assigned to Mo cations with an oxidation state lower than 6+ [26–28], i.e. MoO_2 present a band at 500 nm [27], while this appears at 550 nm in

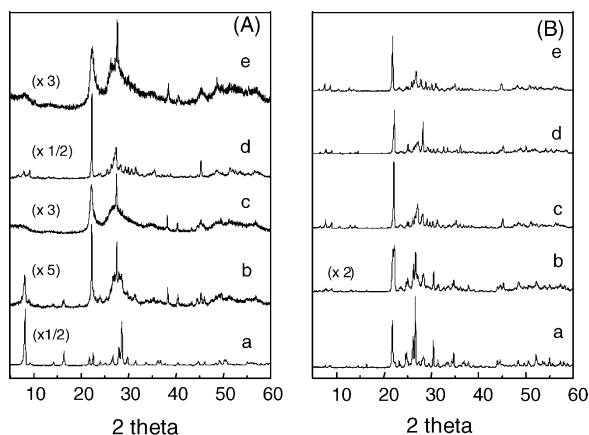


Fig. 1. XRD patterns of Nb-free and Nb-containing MoVTe-oxide samples before (A) and after (B) the heat-treatment: (a) **T6-1**; (b) **T6-1-O**; (c) **T6-2**; (d) **T4-1**; (e) **T4-2**.

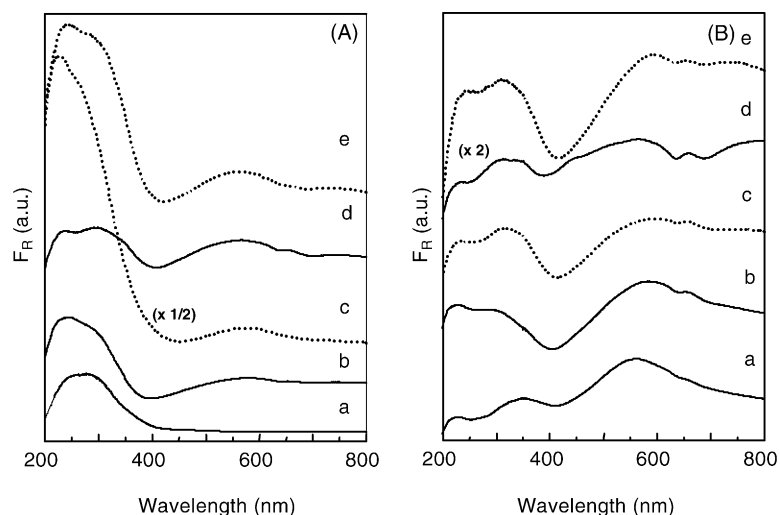


Fig. 2. Diffuse reflectance UV-vis spectra of Nb-free and Nb-containing MoVTe-oxide samples before (A) and after (B) the heat-treatment: (a) **T6-1**; (b) **T6-1-O**; (c) **T6-2**; (d) **T4-1**; (e) **T4-2**.

$\text{TeMo}_5\text{O}_{16}$ [28] and at 585 nm in Mo_9O_{26} [27]. So, the results of Fig. 2B suggest a stronger reduction of Mo-species than that observed in the uncalcined samples, as a consequence of the heat-treatment in N_2 .

Porter et al. [27] proposed a linear correlation between the band frequencies observed in intermediate molybdenum oxides and the number of 4d electrons per cation. According to this, an oxidation state of molybdenum of 5.8 (thus, suggesting the presence of 20% of Mo atoms with oxidation state 5+) could be proposed in our catalysts. This is in good agreement to previously reported EPR results of Mo-V-Te-Nb-O samples prepared by hydrothermal synthesis [10].

The presence of V^{4+} (broad band in the 600–800 nm region) can also be proposed in the heat-treated samples, although according to previous EPR results [10], its presence should be relatively low. However, sample **T4-1** seems to present the highest intensity in the broad band at 600–800 nm, suggesting the highest presence of V^{4+} species in this sample.

XPS results of heat-treated samples are shown in Table 1. The Mo 3d spectra can be fitted in all cases into two components, at binding energies of 231.7 and 232.7 eV, which can be related to Mo^{5+} and Mo^{6+} , respectively [10,30]. As shown in Table 1, similar $\text{Mo}^{6+}/\text{Mo}^{5+}$ surface atomic ratios were observed in our samples, except in the case of **T4-2** sample in which a higher contribution of Mo^{5+} species can be observed. In addition to these, a new component at lower binding energies (230.7 eV), related to a lower oxidation state of the Mo species (Mo^{n+} , $n < 5$), can be observed in samples **T4-2** and **T6-1**.

The V $2p_{3/2}$ core level spectra of catalysts can mainly be fitted into two components at 516.2 and 517.3 eV, which can be related to the presence of V^{4+} and V^{5+} species, respectively [31]. However, the amount of V^{4+} species on the catalyst surface seems to be higher than those observed by diffuse reflectance or EPR [11] in the bulk. In addition to

these, an asymmetry at low BE related to the presence of a component at 515.3 eV has been evidenced in sample **T4-2**, indicating the presence of V^{3+} .

The Te $3d_{5/2}$ core level spectra of the main samples, is composed by only one component at 576.2 eV, which can be related to the presence of Te^{4+} species [30]. However, a slight asymmetry in the high binding energy site related to a component at 577.1 eV, due to the presence of Te^{6+} species, is only observed in sample **T6-1**. The presence of Te^{6+} species in sample **T6-1**, which is not observed in **T6-1-O** or **T6-2** samples, suggest that the presence of oxalic acid in the H_6TeO_6 -containing synthesis gel could favour the reduction of Te^{6+} . Moreover, the appearance of V^{3+} and Mo^{4+} species in sample **T4-2** could be favoured by the presence of oxalic acid in the synthesis gel. The fact that V^{3+} species are not observed in the rest of the studied samples (including those prepared with telluric acid/oxalic acid) suggests that the oxidation state of Te in the precursor and/or the presence of oxalic acid in the synthesis gel have a strong influence on the final oxidation state of Mo, V, and Te in the heat-treated samples. Moreover, the presence of Mo^{4+} species in sample **T6-1**, could be stabilized by the presence of Te^{6+} species in the catalyst.

3.2. Catalytic performance in the selective oxidation of propane

Table 3 shows the catalytic results obtained during the oxidation of propane at 380 °C on Mo-V-Te-O and Mo-V-Te-Nb-O catalysts. Acrylic acid (AA), propene and carbon oxides were the main reaction products obtained during the oxidation of propane. Acetic acid (AcetA) was also observed at high propane conversions but with selectivities lower than 20%.

According to the results presented in Table 3, it can be concluded that the oxidation state of the tellurium compound

used in the hydrothermal synthesis strongly influences the catalytic behaviour of these catalysts. In the case of Nb-free samples, the catalyst prepared from TeO_2 (sample **T4-1**) or with a mixture of telluric acid and oxalic acid (sample **T6-1-O**) present catalytic activities in the propane oxidation higher than that prepared from telluric acid (sample **T6-1**). However, the selectivity to acrylic acid in the three catalysts studied was low, while the selectivity to acetic acid was relatively important.

In the case of Nb-containing samples, the catalytic activity presents an opposite trend than that observed in the Nb-free samples. In this way, the catalyst prepared with H_6TeO_6 (**T6-2**) presented a higher propane conversion than the catalyst prepared with TeO_2 (sample **T4-2**). In addition to this, Nb-containing catalysts present selectivities to acrylic acid higher than Nb-free catalysts, the sample prepared with $\text{H}_6\text{TeO}_6/\text{Nb}$ -oxalate presenting both the highest selectivity and yield of acrylic acid.

Fig. 3 shows the variation of the selectivity to the main reaction products with the hydrocarbon conversion obtained during the oxidation of propane on the most active catalysts, i.e. **T4-1** (Fig. 3A) and **T6-2** (Fig. 3B) at 380 °C. A different influence of the hydrocarbon conversion on the selectivity to acrylic acid was observed in both cases. Thus, yields of acrylic acid of 5 and 36% were achieved over **T4-1** and **T6-2**, respectively, at a hydrocarbon conversion of about 50%.

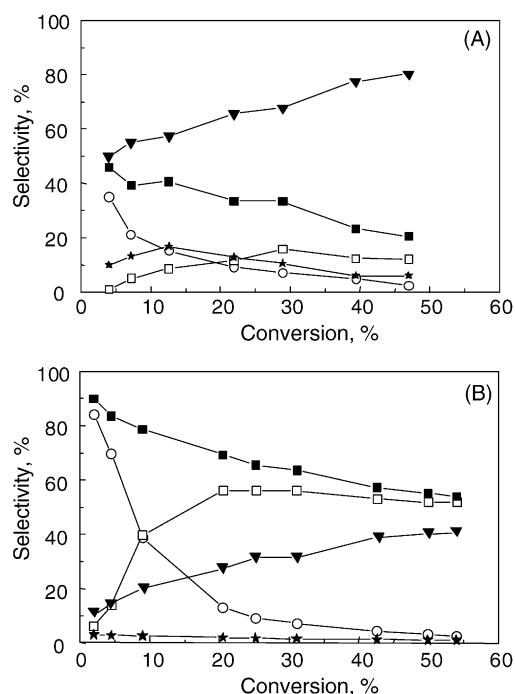


Fig. 3. Variation of the selectivity to the partial oxidation products, during the selective oxidation of propane at 380 °C on samples **T4-1** (A) and **T6-2** (B). Symbols: (■) partial oxidation products, i.e. propene + acrylic acid + acetic acid; (▲) deep oxidation (CO and CO_2); (□) acrylic acid; (○) propene; (★) acetic acid.

However, the less selective catalysts to acrylic acid show a higher selectivity to acetic acid.

So, it can be concluded that the catalytic activity for propane oxidation and the selectivity to acrylic acid depend strongly on the Te-precursors and/or the presence of oxalic acid or Nb oxalate in the synthesis gel.

4. Discussion

The results presented here suggest that the catalytic activity and the nature of crystalline phases depend on the precursors used in the hydrothermal synthesis and could be partially explained by considering some changes of the oxidation states of the main of the elements, as deduced from the XPS results.

It has been proposed that $\text{Te}_2\text{M}_{20}\text{O}_{57}$ phase is the most active and selective phase in the selective oxidation and ammoxidation of propane [4,5,7–9,32,33]. According to our results, this phase can be obtained by hydrothermal synthesis from gels with and without Nb oxalate: (i) $\text{Te}_2\text{M}_{20-x}\text{V}_x\text{O}_{57}$ is obtained by incorporating TeO_2 in the synthesis gel, (ii) $\text{Te}_2\text{M}_{20}\text{O}_{57}$ ($\text{M} = \text{Mo}, \text{V}$ and Nb) is obtained using mixtures of $\text{H}_6\text{TeO}_6/\text{H}_2\text{C}_2\text{O}_4$ or $\text{H}_6\text{TeO}_6/\text{Nb}_2(\text{C}_2\text{O}_4)_5$, respectively. In all of these catalysts, relatively high propane conversions were observed (Table 3).

$\text{Te}_2\text{M}_{20}\text{O}_{57}$ phase is not observed by XRD, however, in the sample obtained from a synthesis gel with telluric acid but in the absence of oxalate anions, which presented a very low activity. The XPS results of this sample before calcination (not shown) and after the calcination step (Table 2) indicate the presence of Te^{6+} ions in addition to Te^{4+} ions, while Te^{6+} ions have been not observed in the rest of the catalysts (including their corresponding uncalcined samples). So, it can be concluded that Te^{4+} ions should be present in the synthesis gel in order to obtain active catalysts for propane oxidation. However, and in addition to the use of TeO_2 in the hydrothermal synthesis [14,15], Te^{4+} ions could

Table 2
XPS of Nb-free and Nb-containing MoVTe-oxide catalysts

Sample	XPS atomic ratio	Surface oxidation states		
		$\text{Mo}^{6+}/\text{Mo}^{5+}$	$\text{V}^{5+}/\text{V}^{4+}$	$\text{Te}^{6+}/\text{Te}^{4+}$
T4-1	$\text{Mo}_1\text{V}_{0.34}\text{Te}_{0.16}$	0.62/0.38	0.20/0.80	0/1
T6-1	$\text{Mo}_1\text{V}_{0.20}\text{Te}_{0.16}$	0.57/0.37 ^a	0.17/0.83	0.15/0.84
T6-1-O^b	$\text{Mo}_1\text{V}_{0.15}\text{Te}_{0.06}$	0.64/0.36	0.21/0.79	0/1
T4-2	$\text{Mo}_1\text{V}_{0.14}\text{Te}_{0.19}\text{Nb}_{0.18}$	0.37/0.61 ^c	0.15/0.72 ^d	0/1
T6-2	$\text{Mo}_1\text{V}_{0.18}\text{Te}_{0.19}\text{Nb}_{0.19}$	0.56/0.44	0.18/0.82	0/1

^a The presence of Mo^{n+} species with an oxidation state lower than 5+ is also observed ($\text{Mo}^{n+}/\text{Mo}^{5+}$ atomic ratio of 0.08/0.37).

^b Oxalic acid instead of Nb oxalate has been incorporated in the synthesis gel.

^c The presence of Mo^{n+} species with an oxidation state lower than 5+ is also observed ($\text{Mo}^{n+}/\text{Mo}^{5+}$ atomic ratio of 0.02/0.61).

^d The presence of V^{3+} species with a $\text{V}^{3+}/\text{V}^{4+}$ ratio of 0.12/0.72 is also observed.

Table 3

Catalytic behaviour in the selective oxidation of propane of Nb-free and Nb-containing MoVTe-oxide catalysts

Sample	W/F ^a	Temperature (°C)	Conversion (%)	Selectivity ^b (%)			
				AA	C ₃ H ₆	AcetA	CO + CO ₂
T4-1	205	380	21.9	15.4	10.8	7.5	66.3
	500	380	46.2	5.7	2.9	17.4	74.0
T6-1	500	380	6.1	15.0	20.1	3.0	61.9
T6-1-O	205	380	11.7	23.7	15.6	11.4	49.3
	500	380	31.4	15.0	4.5	13.0	68.0
T4-2	205	380	8.1	46.2	26.5	2.6	24.7
	500	380	21.1	33.2	8.9	3.6	55.3
T6-2	205	380	17.1	57.0	13.6	5.9	23.5
	500	380	27.9	55.5	2.4	7.7	34.4
	1100	380	58.0	52.0	0.2	8.2	39.6

^a Contact time, W/F, in g_{cat} h mol⁻¹_{C₃H₈}.^b Acrylic acid (AA); acetic acid (AcetA).

also be obtained “in situ” during the hydrothermal synthesis. This is the case of the incorporation of a Te⁶⁺-precursor (telluric acid or an Anderson-type telluromolybdate [16]) in the synthesis gel in the presence of oxalate anions (Nb-oxalate or oxalic acid). In this way, it has been reported that the incorporation of oxalic acid in the synthesis gel can modify the catalytic behaviour of these catalysts in the oxidation [4,11] and ammoxidation [4,5] of propane. Such behaviour seems to be related to changes in the nature of the crystalline phases in the catalyst [5] but also in the oxidation state of each elements.

On the other hand, the catalytic results of Table 3 suggest that the presence of Nb⁵⁺ ions in the catalysts favours higher selectivities to acrylic acid with respect to those Nb-free catalysts. Since the main form to incorporate Nb⁵⁺ ions in the synthesis gel is the use of Nb-oxalate or a mixture of niobic acid/oxalic acid, the synthesis of selective catalysts should be adequately prepared in order to optimise the reduction of Te ions. In this way, the results presented here show that the best active and selective catalysts prepared hydrothermally are those synthesized from mixtures of telluric acid and Nb oxalate in addition to ammonium heptamolybdate and vanadyl sulphate (sample **T6-2**). Although the Nb-containing catalyst prepared from TeO₂ (sample **T4-2**) is also active and selective in propane oxidation, the yield of acrylic acid on this sample is lower than that observed over sample **T6-2**. In these cases some differences in the oxidation state of Mo species on the catalyst surface has been observed. In fact the results in Table 2 suggest a higher reduction of Mo species for the Nb-containing sample prepared from TeO₂ (with a Mo⁶⁺/Mo⁵⁺/Mo⁴⁺ XPS atomic ratio of 0.61/0.37/0.08) than that prepared from H₆TeO₆ (with a Mo⁶⁺/Mo⁵⁺/Mo⁴⁺ XPS atomic ratio 0.56/0.44/0). Mo⁶⁺ species are involved in the selective O-insertion of olefinic intermediate [5,10], while the presence of Mo⁴⁺ could favour deep oxidation reactions [34]. For this reason, the formation and stability of acrylic acid should be favoured in Mo⁴⁺-free catalysts.

5. Conclusions

In conclusion, the nature of Te-precursor used in the hydrothermal synthesis of Nb-free or Nb-containing Mo-V-Te-O catalysts strongly influences their catalytic performance in the selective oxidation of C₃-hydrocarbons. Mo-V-Te-O sample prepared with TeO₂ and Mo-V-Te-Nb-O sample prepared with H₆TeO₆ were the most active catalysts for propane conversion, while Mo-V-Te-O catalyst prepared with H₆TeO₆ and Mo-V-Te-Nb-O catalysts prepared with TeO₂ presented the lowest activity for propane conversion. Moreover, the highest selectivities to acrylic acid were obtained on Nb⁵⁺-containing catalysts.

The best catalytic results of the Mo-V-Te-Nb-O catalysts prepared with H₆TeO₆ can be explained by considering both the formation of Te₂M₂₀O₅₇ (M = Mo, V and Nb) phase with Nb⁵⁺ incorporated in the framework. According to these results, both the formation of the active crystalline phase and the incorporation of Nb⁵⁺ ions can be quite favoured by the presence of oxalate anions and a Te⁶⁺-precursor in the synthesis gel. Te₂M₂₀O₅₇ (M = Mo, V and Nb) phase can also be formed by using TeO₂ and Nb-oxalate, but the presence of oxalate anions in this case could partially favour a higher reduction of V and Mo ions (with the appearance of V³⁺ and Mo⁴⁺ species, in addition to Mo⁶⁺, Mo⁵⁺, V⁵⁺ and V⁴⁺) and, consequently, a decrease of both the catalytic activity and the selectivity to acrylic acid.

A better characterization of the crystalline phases and the evolution of the synthesis gel during the hydrothermal synthesis can help to understand the role of each element in the catalytic behaviour of these catalysts.

Acknowledgment

Financial support from DGICYT in Spain through Project PPQ2003-03946 is gratefully acknowledged.

References

- [1] T. Ushikubo, K. Oshima, A. Kayo, T. Umezawa, K. Kiyono, I. Sawaki, EP Patent 529 853 A2 (1992).
- [2] T. Ushikubo, K. Oshima, A. Kayo, M. Hatano, *Stud. Surf. Sci. Catal.* 112 (1997) 473.
- [3] K. Asakura, K. Nakatani, T. Kubota, Y. Iwasawa, *J. Catal.* 194 (2000) 309.
- [4] H. Tsuji, Y. Koyasu, *J. Am. Chem. Soc.* 124 (2002) 5608.
- [5] R.K. Grasselli, J.D. Burchington, D.J. Buttrey, P. DeSanto, C.G. Lugmair, A.F. Volpe, T. Weingard, *Top. Catal.* 23 (2003) 5.
- [6] (a) T. Ushikubo, H. Nakamura, Y. Koyasu, S. Wajiki, US Patent 5,380,933 (1995);
(b) M. Lin, M.W. Linsen, EP 962 253 (1999);
(c) S. Komada, H. Hinago, M. Kaneta, M. Watanabe, EP Patent 0896809 A1 (1999).
- [7] H. Tsuji, K. Oshima, Y. Koyasu, *Chem. Mater.* 15 (2003) 2112.
- [8] M. Baca, A. Pigamo, J.L. Dubois, J.M.M. Millet, *Top. Catal.* 23 (2003) 39.
- [9] J.M. Oliver, J.M. López Nieto, P. Botella, A. Mifsud, *Appl. Catal. A: Gen.* 257 (2004) 67.
- [10] P. Botella, J.M. López Nieto, B. Solsona, A. Mifsud, F. Márquez, *J. Catal.* 209 (2002) 445.
- [11] P. Botella, B. Solsona, A. Martínez-Arias, J.M. López Nieto, *Catal. Lett.* 74 (2001) 149.
- [12] (a) J.M. López Nieto, P. Botella, M.I. Vázquez, A. Dejoz, *Chem. Commun.* (2002) 1906;
(b) J.M. López Nieto, P. Botella, M.I. Vázquez, A. Dejoz, WO Patent 03/064035 (2003).
- [13] P. Botella, E. García-González, A. Dejoz, J.M. López Nieto, M.I. Vázquez, J.M. González-Calbet, *J. Catal.* 225 (2004) 428.
- [14] W. Ueda, K. Oshihara, *Appl. Catal. A: Gen.* 200 (2000) 135.
- [15] W. Ueda, K. Oshihara, D. Vitry, T. Hirano, Y. Kayashima, *Catal. Surv. Jpn.* 6 (2002) 33.
- [16] J.M. López Nieto, P. Botella, B. Solsona, J.M. Oliver, *Catal. Today* 81 (2003) 87.
- [17] D. Vitry, J.L. Dubois, W. Ueda, *Appl. Catal.* 251 (2003) 411.
- [18] E. García-González, J.M. López Nieto, P. Botella, J.M. González-Calbet, *Chem. Matter.* 14 (2002) 4416.
- [19] C.D. Wagner, L.E. Davis, M.V. Zeller, T.A. Taylor, R.H. Raymond, L.H. Gale, *Surf. Interface Anal.* 3 (1981) 211.
- [20] M. Wark, M. Koch, A. Bückner, W. Grünert, *J. Chem. Soc., Faraday Trans.* 94 (1998) 2033.
- [21] P. Botella, J.M. López Nieto, B. Solsona, *J. Mol. Catal. A: Chem.* 184 (2002) 335, and references therein.
- [22] S. Yuhao, L. Jingfu, W. Enbo, *Inorg. Acta* 117 (1986) 23.
- [23] J.N. Al-Saeedi, V.K. Vasudevan, V.V. Gulians, *Catal. Commun.* 4 (2003) 537.
- [24] J.M.M. Millet, H. Roussel, A. Pigamo, J.L. Dubois, J.C. Jumas, *Appl. Catal. A: Gen.* 232 (2002) 77.
- [25] P. DeSanto, D.J. Buttrey, R.K. Grasselli, C.G. Lugmair, A.F. Volpe, B.H. Toby, T. Vogt, *Top. Catal.* 23 (2003) 23.
- [26] H. Aritani, T. Tanaka, T. Funabiki, S. Yoshida, K. Eda, N. Sotani, M. Kudo, S. Hasegawa, *J. Phys. Chem.* 100 (1996) 19495.
- [27] V.R. Porter, W.B. White, R. Roy, *J. Solid State Chem.* 4 (1972) 250.
- [28] J.C.J. Bart, F. Cariati, A. Sgamellotti, *Inorg. Chim. Acta* 36 (1979) 105.
- [29] E. García-González, J.M. López Nieto, P. Botella, J.M. González-Calbet, *Chem. Mater.* 14 (2002) 4416.
- [30] H. Hayashi, N. Shigemoto, S. Sugiyama, N. Maseoka, K. Saitho, *Catal. Lett.* 19 (1993) 273.
- [31] M. Demeter, M. Newman, W. Reichelt, *Surf. Sci.* 454–456 (2000) 41.
- [32] J. Holmberg, R.K. Grasselli, A. Andersson, *Top. Catal.* 23 (2003) 55.
- [33] D. Vitry, Y. Morikawa, J.L. Dubois, W. Ueda, *Top. Catal.* 23 (2003) 47.
- [34] M. Mezourki, B. Taouk, L. Tessier, E. Bordes, P. Courtine, *Stud. Surf. Sci. Catal.* 75 (1993) 753.